

Microwave-Assisted Synthesis of $\text{Li}_4\text{Ti}_5\text{O}_{12}$ from $\text{TiO}(\text{OH})_2$ and Its Application for Hybrid Capacitors

Byung-Gwan Lee^{1,2}, Hyo-Jin Ahn^{1,*}, and Jung-Rag Yoon^{2,*}

¹Program of Materials Science and Engineering, Convergence Institute of Biomedical Engineering and Biomaterials, Seoul National University of Science and Technology, Seoul 01811, Republic of Korea

²R&D Center, Samwha Capacitor Co., Ltd, Youngin 17118, Republic of Korea

We report two types of spinel $\text{Li}_4\text{Ti}_5\text{O}_{12}$ synthesized from the mixtures of two different nano-sized Ti precursors ($\text{TiO}(\text{OH})_2$ and TiO_2) using microwave heating. The mixed precursors were heated at various temperatures ranging from 450 to 750 °C using microwave heating processing. Spinel $\text{Li}_4\text{Ti}_5\text{O}_{12}$ prepared from $\text{TiO}(\text{OH})_2$ as a Ti precursor exhibits lower synthesis temperature of 550 °C than $\text{Li}_4\text{Ti}_5\text{O}_{12}$ prepared from TiO_2 . Two types of spinel $\text{Li}_4\text{Ti}_5\text{O}_{12}$ obtained from $\text{TiO}(\text{OH})_2$ and TiO_2 were characterized using X-ray diffraction, particle size distribution, and scanning electron microscopy. Hybrid capacitors to evaluate the electrochemical performance of spinel $\text{Li}_4\text{Ti}_5\text{O}_{12}$ were fabricated using activated carbon as a cathode material. $\text{TiO}(\text{OH})_2$ has the advantage of low-temperature synthesis in comparison with rutile or anatase phase TiO_2 , because $\text{TiO}(\text{OH})_2$ possesses a high concentration of defects in the structure. As a result, the rate capability of the hybrid capacitor improved with the decreasing particle size of the $\text{Li}_4\text{Ti}_5\text{O}_{12}$ prepared from $\text{TiO}(\text{OH})_2$ owing to the increasing contact area between electrode and electrolyte, as well as reduced diffusion path of lithium ions. In this study, we demonstrated that the high-rate performance and long-term cycle stability of $\text{Li}_4\text{Ti}_5\text{O}_{12}$ obtained from $\text{TiO}(\text{OH})_2$ for hybrid capacitors. The presented hybrid capacitor could be a competitive candidate for use in promising energy storage devices.

Keywords: $\text{Li}_4\text{Ti}_5\text{O}_{12}$, Lithium Titanate, Metatitanic Acid, Microwave, Hybrid Capacitor.

1. INTRODUCTION

$\text{Li}_4\text{Ti}_5\text{O}_{12}$ is a very promising anode material for hybrid capacitors and Li-ion batteries because it does not undergo structural change during the charge/discharge process.^{1–4} This characteristic ensures a long life cycle and excellent cycle performance. The $\text{Li}_4\text{Ti}_5\text{O}_{12}$ inserts three lithium ions per formula unit, with a theoretical capacity of 175 mAhg^{-1} . It shows a voltage flat at 1.5 V versus Li/Li^+ , above the reduction potential of most electrolyte solvents.⁵ Therefore, solid electrolyte interphase (SEI) layers owing to the reduction of electrolyte on the electrode surface would be less likely to form. For the same reason, the formation of metallic lithium during the discharge process can also be avoided. It is generally agreed that $\text{Li}_4\text{Ti}_5\text{O}_{12}$ is suitable for good reversibility and structure stability over a long-term cycle.⁶ Despite these advantages, a potential drawback of $\text{Li}_4\text{Ti}_5\text{O}_{12}$ is its poor electrical conductivity ($10^{-13} \text{ Scm}^{-1}$).⁷ As a result, anodes made

from $\text{Li}_4\text{Ti}_5\text{O}_{12}$ show large polarization resistance at high charge/discharge rates. To overcome this problem, the following have been attempted: surface coating with carbon, doping with metal or non-metal ions to increase the intrinsic electronic conductivity, and decreasing the grain size via advanced synthesis techniques to reduce the diffusion distance.^{8–10}

Traditionally, $\text{Li}_4\text{Ti}_5\text{O}_{12}$ powders have been synthesized by a solid-state reaction that involves mechanical mixing of TiO_2 and Li_2CO_3 precursors, heating at higher temperatures ranging from 750 to 1100 °C.^{11–15} Such high calcination temperatures not only coarsened the powders but also increased the lithium evaporation rate. In these conventional methods involving resistant, radiation, and convection heating, the thermal energy is absorbed on the material surface and then transferred towards the inside through thermal conductivity. On the other hand, for microwave heating, the electromagnetic energy is absorbed by the material as a whole owing to microwave-matter coupling and deep penetration. Then, it is converted to heat

*Authors to whom correspondence should be addressed.

through dielectric (ceramics) or magnetic permittivity/eddy currents (metals) loss mechanisms.¹⁶ Therefore microwave heating allows synthesis to be done faster and cleaner with reduced solvent consumption due to the energy conversion and no thermal conductivity mechanism. In this study, we adopted a microwave-assisted synthesis process with a high degree of particle size control and morphology in rapid time because this is a highly economical and simple method. Herein, we demonstrate the electrochemical properties of $\text{Li}_4\text{Ti}_5\text{O}_{12}$ as a lithium intercalation host for hybrid capacitors using spinel $\text{Li}_4\text{Ti}_5\text{O}_{12}$ powders prepared by microwave-assisted synthesis. $\text{TiO}(\text{OH})_2$ possess a high concentration of defects that lead to lower synthesis temperature. Therefore, $\text{Li}_4\text{Ti}_5\text{O}_{12}$ powders were synthesized from $\text{TiO}(\text{OH})_2$ and Li_2CO_3 . To find out the differences between $\text{TiO}(\text{OH})_2$ and TiO_2 as Ti precursor, $\text{Li}_4\text{Ti}_5\text{O}_{12}$ was also synthesized using TiO_2 and Li_2CO_3 .

2. EXPERIMENTAL DETAILS

2.1. Sample Synthesis

$\text{TiO}(\text{OH})_2$ and TiO_2 was obtained from COSMO CHEMICAL(KOREA) and SHOWA DENKO(JAPAN), respectively. Two types of spinel $\text{Li}_4\text{Ti}_5\text{O}_{12}$ were synthesized: from $\text{TiO}(\text{OH})_2$ and TiO_2 as Ti precursor; and from Li_2CO_3 as Li precursor. Stoichiometric amounts of Ti and Li, with a 5:4 rate, were mixed in ethanol (99.9%). After ball milling for 12 h, the mixed slurry was dried at 80 °C. To obtain the spinel $\text{Li}_4\text{Ti}_5\text{O}_{12}$, the mixed precursors were heat-treated from 450 to 750 °C by microwave heating for 5 min under air atmosphere. Microwave power was generated at 2.45 GHz. The X-ray diffraction (XRD) of the samples were recorded with $\text{Cu K}\alpha$ ($\lambda = 1.5406 \text{ \AA}$) radiation in the diffraction angle of 2θ from 10 to 80° at a scan rate of 5° min^{-1} . The particle size distribution (PSD) was identified by laser particle size analyzer (HORIBA LA-900). The morphologies of the samples were characterized by scanning electron microscopy (SEM, JEOL JSM-7500F).

2.2. Preparation of Hybrid Capacitor and Electrochemical Measurements

Cylindrical hybrid capacitors ($\Phi 22 \times 45 \text{ mm}$) were fabricated by using activated carbon (BET: $\sim 1700 \text{ m}^2/\text{g}$, ash contents $< 400 \text{ ppm}$, and average particle size of $10 \mu\text{m}$) as positive electrode and $\text{Li}_4\text{Ti}_5\text{O}_{12}$ as negative electrode. The $\text{Li}_4\text{Ti}_5\text{O}_{12}$ electrodes of the hybrid capacitors were prepared by mixing 80% $\text{Li}_4\text{Ti}_5\text{O}_{12}$ powders, 10% conductive carbon black (Super-P Li), and 10% polyvinylidene fluoride (PVdF) as a binder. *N*-methyl pyrrolidone (NMP) was used as a solvent. The slurry obtained from the mixture was coated by an aluminum current collector and dried at 150 °C to remove the NMP solvent. The activated carbon electrodes were prepared by mixing activated carbon, conductive carbon black, and polytetrafluoroethylene (PTFE) as a binder in weight ratio of 75:15:10. The coated electrodes were cut to $35 \times 65 \text{ cm}$ and then wound together

with cellulose separator. Electrochemical properties of the $\text{Li}_4\text{Ti}_5\text{O}_{12}$ with different particle sizes were examined in hybrid capacitors in combination with an activated carbon positive electrode.

The positive and negative electrodes were based on an active material weight ratio of 4:1. The balancing ratio was calculated using specific capacity of 40 mAhg^{-1} for the activated carbon and specific capacity of 160 mAhg^{-1} for $\text{Li}_4\text{Ti}_5\text{O}_{12}$. The electrolyte was 1 M solution of LiPF_6 in acetonitrile. The electrochemical performance was evaluated in the potential range from 1.5 to 2.8 V at room temperature using a programmable multichannel battery tester (Arbin Instruments).

3. RESULTS AND DISCUSSION

Figure 1(a) shows the XRD patterns of the microwave treated powders from TiO_2 and Li_2CO_3 . Heating temperatures of the precursors were at 450, 550, 650 and 750 °C for 5 min in air. The diffraction peaks of weak intensity,

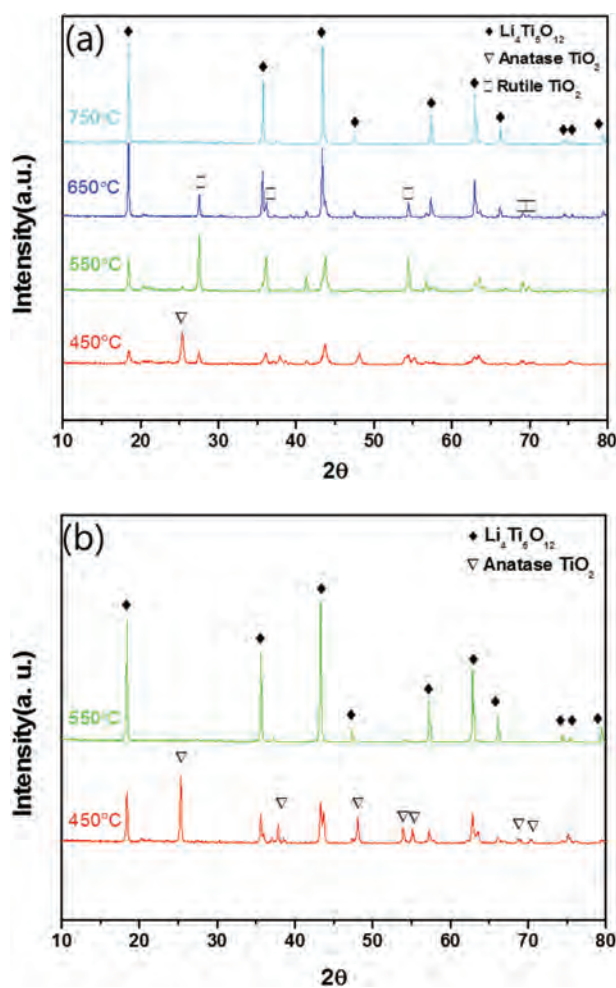


Figure 1. X-ray diffraction patterns of the samples prepared by microwave heating at various temperatures in air for 5 min. (a) $\text{TiO}_2 + \text{Li}_2\text{CO}_3$ and (b) $\text{TiO}(\text{OH})_2 + \text{Li}_2\text{CO}_3$.

assigned to the spinel-type $\text{Li}_x\text{TiO}_{2+x/2}$ phase, along with the diffraction peaks of the main anatase TiO_2 phase were observed at 450 °C. However, no lithium related phase was detected, suggesting phase reaction between TiO_2 and the Li by incorporating Li^+ into the TiO_2 lattice with the formation of a spinel-type $\text{Li}_x\text{TiO}_{2+x/2}$ composite oxide.^{6,17} The peak intensity of the rutile TiO_2 phase relatively increased with increasing heating temperature. The rutile phase with weak peak intensity was observed between 450 and 650 °C. At 750 °C, only the spinel $\text{Li}_4\text{Ti}_5\text{O}_{12}$ was detected, suggesting synthesis of a pure $\text{Li}_4\text{Ti}_5\text{O}_{12}$ phase. On the other hand, according to the $\text{Li}_4\text{Ti}_5\text{O}_{12}$ cubic spinel phase structure, spinel- $\text{Li}_4\text{Ti}_5\text{O}_{12}$ was successfully synthesized from $\text{TiO}(\text{OH})_2$ and Li_2CO_3 at 550 °C.

As shown in Figure 1(b), no peak characteristic of any impurities (TiO_2) is found in samples synthesized at 550 °C. However, the synthesis process from $\text{TiO}(\text{OH})_2$ precursor is different from TiO_2 . The microwave irradiation breaks the Ti complex and a large amount of OH^- ligands present. The strong interaction between OH^- group and protonated surfaces results in Ti–O–Ti bridge. It is expected to generate nuclei of anatase type that serves poly condensation and nucleation of TiO_2 .¹⁸ Therefore, pure $\text{Li}_4\text{Ti}_5\text{O}_{12}$ phase could be synthesized from $\text{TiO}(\text{OH})_2$ precursor at 550 °C.

Figure 2(a) shows the morphology of the $\text{Li}_4\text{Ti}_5\text{O}_{12}$ powders obtained from TiO_2 and Li_2CO_3 at 750 °C. The presence of the $\text{Li}_4\text{Ti}_5\text{O}_{12}$ nanocrystallite aggregates assembled by agglomerated nanoparticles with sizes was observed. The $\text{Li}_4\text{Ti}_5\text{O}_{12}$ nanocrystallite aggregates show the sharp edges. There are obvious differences of particle morphology comparing $\text{Li}_4\text{Ti}_5\text{O}_{12}$ from $\text{TiO}(\text{OH})_2$ and from Li_2CO_3 . As shown in Figure 2(b), the surface morphology of the $\text{Li}_4\text{Ti}_5\text{O}_{12}$ synthesized by $\text{TiO}(\text{OH})_2$ precursor exhibits more porous structure and smaller particle size than $\text{Li}_4\text{Ti}_5\text{O}_{12}$ synthesized by TiO_2 . In other words, in accordance with PSD data of Table I, the secondary particle size of $\text{Li}_4\text{Ti}_5\text{O}_{12}$ prepared from $\text{TiO}(\text{OH})_2$ is smaller than that of $\text{Li}_4\text{Ti}_5\text{O}_{12}$ prepared from TiO_2 . Grain growth occurs when packed Ti and Li precursor particles are heated over synthesis temperature where there is sufficient atomic motion to grow bonds between the particles. The conditions that induce grain growth of $\text{Li}_4\text{Ti}_5\text{O}_{12}$ depend

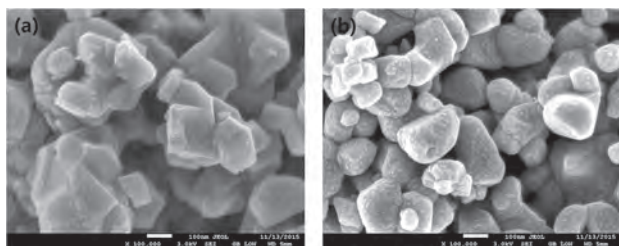


Figure 2. SEM images of (a) the microwave treated powders from TiO_2 and Li_2CO_3 at 750 °C, (b) $\text{TiO}(\text{OH})_2$ and Li_2CO_3 at 550 °C for 5 min in air atmosphere.

Table I. PSD of $\text{Li}_4\text{Ti}_5\text{O}_{12}$ synthesized from TiO_2 and $\text{TiO}(\text{OH})_2$ precursors.

Materials	$D_{(10)}$	$D_{(30)}$	$D_{(50)}$	$D_{(70)}$	$D_{(90)}$
$\text{TiO}_2 + \text{Li}_2\text{CO}_3$	4.68	13.21	21.73	31.96	55.05
$\text{TiO}(\text{OH})_2 + \text{Li}_2\text{CO}_3$	1.86	7.21	17.40	27.64	47.90

on the precursor, and its reaction temperature. As a result, the surface morphology and particle size were affected by the lower synthesis temperature of $\text{TiO}(\text{OH})_2$.

Figure 3 shows the PSD of the $\text{Li}_4\text{Ti}_5\text{O}_{12}$ by microwave heating. Its analysis confirmed the mean aggregate diameter. Its stability even after ultra-sonication, indicated fusion of the primary crystals.¹⁹ PSD of $\text{Li}_4\text{Ti}_5\text{O}_{12}$ synthesized from TiO_2 and $\text{TiO}(\text{OH})_2$ are listed in Table I. In order to improve the high rate capability of $\text{Li}_4\text{Ti}_5\text{O}_{12}$ by reducing diffusion path, the synthesis at lower temperature to restrain the grain growth of $\text{Li}_4\text{Ti}_5\text{O}_{12}$ is needed because the particle size strongly affect high rate performance during the charge and discharge processes.

Figure 4 shows the discharge curves of the hybrid capacitor (denoted as TiO_2 -LTO cell) using $\text{Li}_4\text{Ti}_5\text{O}_{12}$ synthesized from TiO_2 and Li_2CO_3 precursors; and the hybrid capacitor (denoted as $\text{TiO}(\text{OH})_2$ -LTO cell) using $\text{Li}_4\text{Ti}_5\text{O}_{12}$ synthesized from $\text{TiO}(\text{OH})_2$ and Li_2CO_3 precursors at current density of 1 A. The discharge capacities of $\text{TiO}(\text{OH})_2$ -LTO cell and TiO_2 -LTO cell are 81.4 and 82.5 mAh, respectively.

In order to find out the difference between discharge capacity and capacitance, hybrid capacitors capacitance was calculated at voltage ranging from 1.5 V to 2.7 V, considering a voltage flat (1.5 V) of LTO and IR-drop of cells. The capacitance of TiO_2 -LTO cell and $\text{TiO}(\text{OH})_2$ -LTO cell were recorded at 264 and 266F, respectively. Both capacity and capacitance presented no big difference between

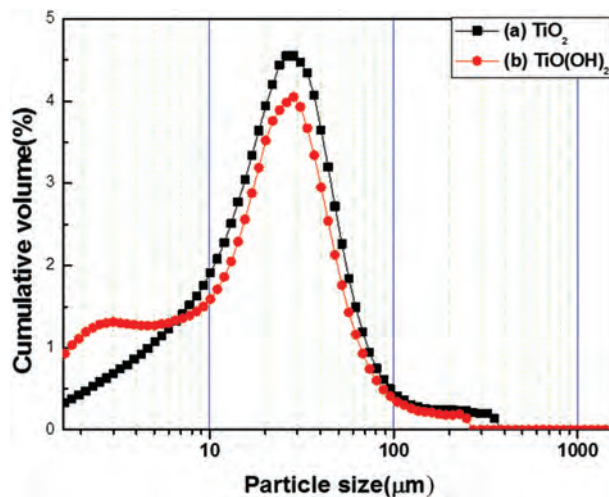


Figure 3. Particle size distribution of the $\text{Li}_4\text{Ti}_5\text{O}_{12}$ powders synthesized from (a) TiO_2 and Li_2CO_3 at 750 °C, and (b) $\text{TiO}(\text{OH})_2$ and Li_2CO_3 at 550 °C.

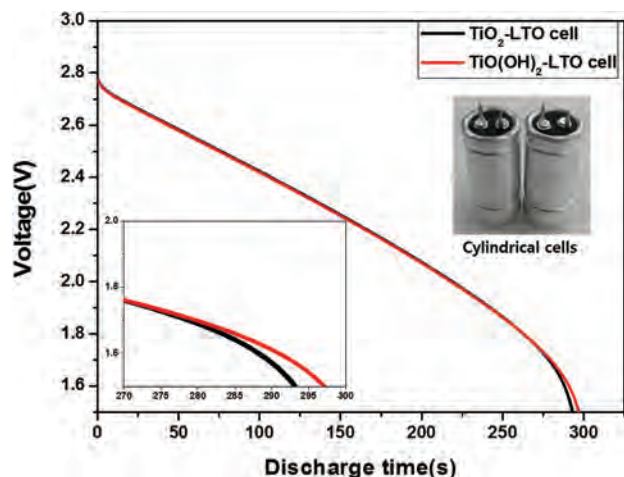


Figure 4. Discharge curves of hybrid capacitors using $\text{Li}_4\text{Ti}_5\text{O}_{12}$ powders from TiO_2 and Li_2CO_3 at 750°C , and from $\text{TiO}(\text{OH})_2$ and Li_2CO_3 at 550°C as anode material. The cells were charged and discharged at 1 A.

TiO_2 -LTO and $\text{TiO}(\text{OH})_2$ -LTO cells at a current density of 1 A.

To investigate the rate capability of TiO_2 -LTO and $\text{TiO}(\text{OH})_2$ -LTO cells, various current densities were applied from 1 to 20 A, as shown in Figure 5.

For both samples, the discharge capacities decrease gradually while the current density increases. However, the $\text{TiO}(\text{OH})_2$ -LTO cell demonstrates remarkably improved rate capability and reversible capacity, especially at 20 A. $\text{TiO}(\text{OH})_2$ -LTO cell displays higher rate capabilities than TiO_2 -LTO cell. The discharge capacities of $\text{TiO}(\text{OH})_2$ -LTO and TiO_2 -LTO cells at 20 A are 62.1 and 55.8 mAh, respectively. We consider this relatively large capacity and high-rate capability due to $\text{Li}_4\text{Ti}_5\text{O}_{12}$ particle microstructure and its particle size prepared by $\text{TiO}(\text{OH})_2$.

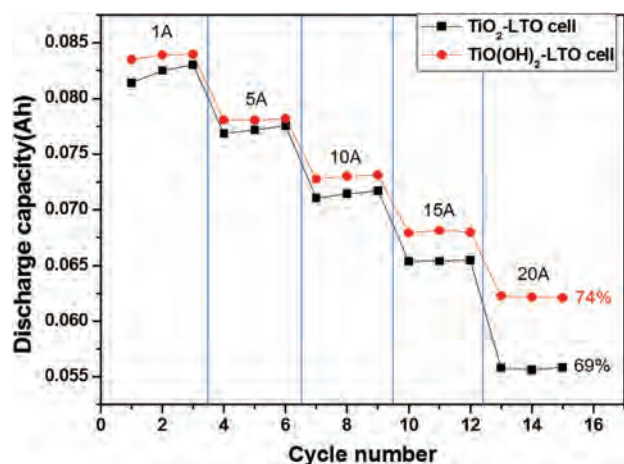


Figure 5. Discharge rate capabilities of hybrid capacitors using $\text{Li}_4\text{Ti}_5\text{O}_{12}$ powders from TiO_2 and Li_2CO_3 at 750°C , and from $\text{TiO}(\text{OH})_2$ and Li_2CO_3 at 550°C as anode material. The cells were charged and discharged at various current rates varying from 1 to 20 A.

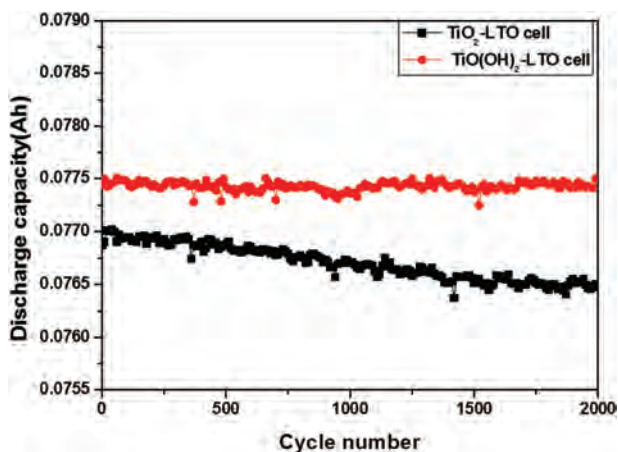


Figure 6. Cycle performance of hybrid capacitors using $\text{Li}_4\text{Ti}_5\text{O}_{12}$ powders from TiO_2 and Li_2CO_3 at 750°C , and from $\text{TiO}(\text{OH})_2$ and Li_2CO_3 at 550°C as anode material. The cells were charged and discharged at 5 A.

The particle size reduction of $\text{Li}_4\text{Ti}_5\text{O}_{12}$ by microwave causes faster kinetics of Li ions.²⁰ Generally, the electrochemical performance of a cell depends on Li^+ diffusion length and diffusion coefficient. Smaller particles promote shorter pathways for Li ions diffusion and result in better rate capability.²¹ Also, the porous structure of the $\text{Li}_4\text{Ti}_5\text{O}_{12}$ prepared from $\text{TiO}(\text{OH})_2$ as mentioned in Figure 2 is beneficial for electrolyte penetration and increases the contact area between the $\text{Li}_4\text{Ti}_5\text{O}_{12}$ and electrolyte.

Figure 6 shows the cycle performance of hybrid capacitors at a current of 5 A. The initial reversible specific capacity of $\text{TiO}(\text{OH})_2$ -LTO and TiO_2 -LTO cells are 77.4 and 76.8 mAh, respectively. After 2,000 cycles, $\text{TiO}(\text{OH})_2$ -LTO cell keeps the discharge capacity of 77.3 mAh. It has great cyclability with almost no capacity fading and exhibits capacity retention of 99.87% after 2,000 cycles, indicating a cycling performance superior to TiO_2 -LTO cell. At a high current density of 5 A, the improved cycle performance of $\text{TiO}(\text{OH})_2$ -LTO cell was attributed to the enlarged surface area, which compensated for the slow lithium ion diffusivity in the solid, suggesting good stability of the $\text{Li}_4\text{Ti}_5\text{O}_{12}$ synthesized from $\text{TiO}(\text{OH})_2$ precursor for hybrid capacitors. As a result, we demonstrate that spinel $\text{Li}_4\text{Ti}_5\text{O}_{12}$ with good crystallinity and 100 nm sized primary particles can be synthesized by microwave heating and $\text{TiO}(\text{OH})_2$ precursor for hybrid capacitors.

4. CONCLUSION

We presented a technology to prepare the nanosized $\text{Li}_4\text{Ti}_5\text{O}_{12}$ by using $\text{TiO}(\text{OH})_2$ as a Ti precursor. Spinel $\text{Li}_4\text{Ti}_5\text{O}_{12}$ powders were successfully obtained with homogeneity, porous structure, and small particle-size distribution by microwave heating. The average particle size is between 100 to 200 nm and the $\text{Li}_4\text{Ti}_5\text{O}_{12}$ powders from $\text{TiO}(\text{OH})_2$ and TiO_2 have a discharge capacity of 77.4 and 76.8 mAh, respectively, at 5 A. The $\text{TiO}(\text{OH})_2$ -LTO

cell show much better rate capability than TiO_2 -LTO cell. Even at 20 A, the $\text{TiO}(\text{OH})_2$ -LTO cell also keeps 74% of capacity compared with 1 A. The cyclability of $\text{TiO}(\text{OH})_2$ -LTO cell over 2,000 cycles exhibits capacity retention of 99.87%. The excellent rate capability and cycling performance are mainly attributed to the small particle size and good crystallinity of $\text{Li}_4\text{Ti}_5\text{O}_{12}$ prepared by $\text{TiO}(\text{OH})_2$ at 550 °C. It indicates that the electrochemical performance of hybrid capacitor depends on the $\text{Li}_4\text{Ti}_5\text{O}_{12}$ properties.

Acknowledgment: This study was supported by R&D Convergence Program of MSIP (Ministry of Science, ICT and Future Planning) and NST (National Research Council of Science and Technology) of Republic Korea (Grant CAP-13-2-ETRI).

References and Notes

1. T. Ohzuku, A. Ueda, and N. Yamamoto, *J. Electrochem. Soc.* 142, 1431 (1995).
2. K. Zaghib, M. Simoneau, M. Armand, and M. Gauthier, *J. Power Sources* 81, 300 (1999).
3. J. M. Tarascon and M. Armand, *Nature* 414, 359 (2001).
4. A. Riduan, M. Faisal, and G. S. Chung, *Trans. Elect. Electron. Mater.* 13, 125 (2012).
5. D. Peramunage and K. M. Abraham, *J. Electrochem. Soc.* 145, 2609 (1998).
6. T. Yuan, R. Cai, R. Ran, Y. Zhou, and Z. Shao, *J. Alloys Compd.* 505, 367 (2010).
7. K. M. Colbow, J. R. Dahn, and R. R. Haering, *J. Power Sources* 26, 397 (1989).
8. D. Capsoni, M. Bini, V. Massarotti, P. Mustarelli, S. Ferrari, G. Chiodelli, M. C. Mozzati, and P. Galinetto, *J. Phys. Chem. C* 113, 19664 (2009).
9. L. Zhao, Y.-S. Hu, H. Li, Z. Wang, and L. Chen, *Adv. Mater.* 23, 1385 (2011).
10. L. Shen, C. Yuan, H. Luo, X. Zhang, K. Xu, and F. Zhang, *J. Mater. Chem.* 21, 761 (2011).
11. H. Zhao, Y. Li, Z. Zhu, J. Lin, Z. Tian, and R. Wang, *J. Electrochim. Acta* 53, 7079 (2008).
12. T. Ohzuku, A. Ueda, and N. Yamamoto, *J. Electrochem. Soc.* 142, 1431 (1995).
13. K. Zaghib, M. Armand, and M. Gauthier, *J. Electrochem. Soc.* 145, 3135 (1998).
14. K. Zaghib, M. Simoneau, M. Armand, and M. Gauthier, *J. Power Sources* 81, 300 (1999).
15. Y. Hao, Q. Lai, J. Lu, H. Wang, Y. Chen, and X. Ji, *J. Power Sources* 158, 1358 (2006).
16. D. Agrawal, *Sohn International Symposium*, San Diego, California, USA, August (2006), p. 183.
17. X. L. Yao, S. Xie, C. H. Chen, Q. S. Wang, J. H. Sun, Y. L. Li, and S. X. Lu, *Electrochim. Acta* 50, 4076 (2005).
18. V. V. Kondalkar, S. S. Mali, N. B. Pawar, R. M. Mane, S. Choudhury, C. K. Hong, P. S. Patil, S. R. Patil, P. N. Bhosale, and J. H. Kim, *Electrochim. Acta* 143, 89 (2014).
19. D. Pasquiera, C. C. Huang, and T. Spitler, *J. Power Sources* 186, 508 (2009).
20. J. H. Lee, H. K. Kim, E. Baek, M. Pecht, S. H. Lee, and Y. H. Lee, *J. Power Sources* 301, 348 (2016).
21. L. Kavan, J. Prochazka, T. M. Spitler, M. Kalbac, M. Zukalova, T. Drezen, and M. Gratzel, *J. Electrochem. Soc.* 150, A1000 (2003).

Received: 31 December 2015. Accepted: 21 March 2016.